BMC Plant Biology

RESEARCH

Open Access

Comparative physiological and cytological analysis, and omics approach provide clues to the coloring mechanism of the pumpkin yellow stems

Liting Deng[1], Jianning Luo[1], Haibin Wu[1], Xiaoxi Liu[1], Gangjun Zhao[1], Hao Gong[1], Xiaoming Zheng[1], Chaoqun Ni[1,2], Xueting Wang[1] and Junxing Li[1*]

Abstract

Background The abnormal chloroplast and pigment accumulation could lead to plant yellowing. However, the plant tissue chlorisis is species-specific and could display various phenotypes due to the genetic and environmental impacts. The molecular mechanisms underlying the plant stem yellowing are less understood than the flower or leaf coloring mechanisms. Herein, the physiological, cytological, transcriptome analysis, along with genome-wide association study (GWAS) were integrated to illustrate the processes relevant to pumpkin stem coloring.

Results Similar yet different variations were discovered in the pumpkin yellow stems. Low content of photosynthetic pigments, and impaired chloroplast thylakoid membrane were identified in the pumpkin yellowing stems, together with the presence of plastoglobules and starch grains. Elevated expression of genes in catabolism of chlorophylls and carotenoids was found in yellow stems, which may result in the failed accumulation of pigments and pumpkin stem chlorisis. Concurrently, increased expression of genes in chloroplast development, antioxidant protection, photosynthesis, and ribosome were found, which may act as compensation mechanisms for chloroplast defects. The integrated analysis of transcriptome and GWAS identified the up-regulated proteases and decreased kinesins in yellow stems, which could result in the breakdown of thylakoid systems, and the disability of photosynthetic pigments accumulation. Additionally, transcription factors could be involved in the regulation of the specific color change in pumpkin stems.

Conclusions These findings provide clues into the molecular mechanisms of stem yellowing, and will facilitate the exploration of candidate targets as markers or genetic improvement through molecular breeding.

Keywords Pumpkin, Chlorisis, Chloroplast, Chlorophyll, Carotenoid, Photosynthesis

*Correspondence:
Junxing Li
lijunxing@gdaas.cn
[1]Guangdong Key Laboratory for New Technology Research of Vegetables, Vegetable Research Institute, Guangdong Academy of Agricultural Sciences, Jinying Road No.66, Guangdong 510640 Guangzhou, China
[2]Guangdong Provincial Key Laboratory of Protein Function and Regulation in Agricultural Organisms, College of Life Sciences, South China Agricultural University, Guangzhou 510642, Guangdong, China

Background

Chloroplasts are essential organelles for plant photosynthesis and many crucial metabolic pathways. Photosynthetic pigments, including chlorophylls and carotenoids, are mostly produced in chloroplast, and then stored in specific tissues [1]. Chlorophylls take charge of the light absorption and excitation energy transfer within the photosynthetic complexes. Carotenoid molecules localized in the thylakoid membrane as vital antioxidants and photo-protectors [2–4]. The chlorophyll–carotenoid–protein complexes are formed in thylakoids coupled with the light-harvesting antenna of photosystem I (PSI) and photosystem II (PSII). The structure is vital to the light-harvesting complexes stabilization, energy transfers, photochemical redox reactions, photo-protection, and the PSII function. Chloroplast defects in plant tissues generally accompany with the loss of chlorophylls and carotenoids [5–7]. The chlorophyll-carotenoid-proteins break down in thylakoids during the plant yellowing or senescence [8]. However, the chlorisis phenotypes are various and species-dependent, which makes them valuable resources for exploring the chloroplast development, photosynthesis, chlorophyll and carotenoid metabolism.

The functional chloroplast and photosynthesis establishment rely on two precise regulatory phases, which are controlled by different mechanisms [9]. The initial phase is light-induced rapid changes in gene expression, metabolite production, chlorophyll accumulation and plastid structure. In the second phase, chloroplast activation-triggered signal is required for the full transition to a functional chloroplast. Dramatic gene expression changes could happen in the nuclear during the process. The signal makes the plant coordinate and synchronize the expression of photosynthetic genes from the nuclear and chloroplast genomes [9]. Pentatricopeptide repeat proteins (PPR), are one of the largest nuclear-encoded protein families in higher plants. They are involve in the post-transcriptional regulation of chloroplast genes and have impressive effects on chloroplast biogenesis and function, consequently, on the photosynthesis through the cooperative action of RNA metabolism [10]. Filamentation temperature-sensitive H (FtsH) and mitochondrial transcription termination factor (mTERF) are positive regulators of the chloroplast development [5]. Protochlorophyllide reductase (POR) and stay-green protein (SGR) are involved in chlorophyll biosynthesis. It is reported that the chlorophyll content decreased in *por* and *sgr* mutations of the tea (Li et al., 2019; Ma et al., 2018). *NOL* and *HCAR* are two vital genes during the chlorophyll degradation. They convert chlorophyll b to chlorophyll a. *PDS* and *ZDS* are involved in carotenoid metabolism, and gene silencing could induce the albino phenotypes (Wang et al., 2020; Zhang et al., 2021).

Notably, chloroplast genome encodes about half of subunits of PSI and PSII, cytochrome b6/f complex, NADH dehydrogenase-like complex (NDH), and ATP synthase (ATPase) in thylakoid membranes. These genes mediate electron transport and ATP synthesis during photosynthesis [11]. Besides, plants have chloroplast ribosomes. They are essential for the translation of the core proteins involved in photosynthesis [12, 13]. Many of the subunits are synthesized on the thylakoid-bound ribosomes and inserted into the thylakoid membrane [11]. A bacterial-type chloroplast ribosome 70S consisting of a 50S large subunit and a 30S small subunit, is vital to the chloroplast translation machinery and protein biosynthesis [13]. Mutations of genes involved in the associated processes could result in the abnormal chloroplast structure, decreased photosynthetic capacity, tissue color changes at different degrees or growth delay [5, 14].

Besides, photoexcitation of free chlorophylls, carotenoids and associated metabolic intermediates could generate reactive oxygen species resulting in color variation in plants. Phytohormone signalling, mainly including ethylene, abscisic acid (ABA), and jasmonic acid (JA), could mediate chlorophyll degradation [15]. Therefore, chloroplast development and pigment formation are progressive processes, and regulated by diverse clues [15]. Pumpkin is one of the most important *Cucurbita* crops in the world. Either pumpkin fruits, seeds, or leaves are favourable food with valuable nutrients, including carotenoids, proteins, monounsaturated or polyunsaturated fatty acids, and amino acids [16, 17]. Stem development is vital to the absorption and transfer of nutrients. Stem yellowing may impact plant growth and crop yield. To the best of our knowledge, few studies explored the molecular mechanisms related to the stem yellowing in the pumpkin. In the study, we characterized phenotypes of different pumpkin materials, and selected three varieties of which stems separately displayed regular green, yellow, and pale yellow colors for further analysis. Comprehensive comparison analysis was applied at physiological, cytological, and gene transcriptional levels, to explore molecular mechanisms of the pumpkin stem coloring. Genome-wide association study (GWAS) was integrated with transcriptome data to discover factors involved in stem yellowing. Findings in the study will be valuable for understanding the pumpkin stem coloring mechanism and associated molecular breeding.

Materials and methods

Pumpkin materials planting and sampling

Pumpkin varieties P11, P144 and P64, which beong to *Cucurbita moschata*, were chosen as the experimental materials. They are the high-generation selfed progenies constructed by the Vegetable Research Institute, Guangdong Academy of Agricultural Sciences, and separately

display green, yellow and pale yellow colors. Three varieties display green and healthy leaves, and normal fruit development. Firstly, seeds were soaked at 50℃ for four hours before keeping in the incubator at 30℃. After two days in the dark, the germinated seeds were nursed in seedling trays (nutrient soil: perlite: vermiculite = 5:1:1). Seedlings with three true leaves were transplanted to the field (Baiyun experimental base, Guangzhou, China), and cultivated until two months old. Following, mature (S1, S2 and S3) and young stems (YS1, YS2 and YS3) were separately collected from P11, P144 and P64 for the subsequent physiological measurement and transcriptome analysis. Three biological replicates were included for each analysis. In addition, mature stem sections from different materials were carefully harvested and immediately fixed for ultrastructure observation. Besides, 103 *Cucurbita moschata* accessions (Supplementary Table 1) with varied stem color phenotypes were investigated. Fresh leaves were collected for sequencing and genome-wide association study (GWAS) to identify the genetic variants of the associated trait.

Measurement of photosynthetic pigments

A half gram of stems was ground to powder. Pigments were fully extracted using 10 mL of 95% ethanol in the dark. The homogenate was filtrated, and the solution with pigments was collected. The absorbance of chlorophyll a, chlorophyll b and carotenoids was separately determined at 665, 649, and 470 nm wavelengths, with 95% ethanol as the control [7].

Examination of stem sections through transmission electron microscopy

The fresh stem was carefully cut into small pieces (2 mm × 2 mm) using the sharp blade and immediately fixed in the electron microscope fixative with 2% glutaraldehyde in 100 mM phosphate buffer (pH 7.0) at 4℃. After post-fix with 1% osmium tetroxide in 100 mM phosphate buffer (pH 7.4) under dark, tissue was dehydrated using an ethanol gradient series (30%, 50%,70%, 80%, 90%, 95%, and 100%), ethanol/acetone solutions with three different concentrations (3:1, 1:1 and 1:3), and pure acetone. Samples were then penetrated and embedded in EmBed 812 resin. Sections were cut on the Leica UC7 ultramicrotome (Leica, Germany), then stained with 2% uranium acetate saturated alcohol solution and 2.6% lead citrate. The stained section was observed under the HT7800 transmission electron microscope (Hitachi, Japan), and images were captured.

RNA extraction, library construction, and sequencing

RNA was extracted using the Trizol reagent (TaKaRa, Japan). RNA concentration was measured using the Qubit 2.0 fluorometer (Thermo Fisher Scientific, MA, USA). The integrity and purity of RNA were assessed through the agarose gel electrophoresis, and the quality was further verified using Agilent 2100 Bioanalyzer (Agilent, CA, United States). Following, the cDNA library was constructed and validated through quality control assays. Library concentration and size distribution were separately examined through Qubit dsDNA high sensitivity assay and Agilent ScreenTape assay. Molarities were calculated and libraries were normalized using Kapa BioSystems qPCR method before pooling and sequencing on the Illumina platform [17].

Data analysis of RNA-sequencing

Sequencing data is available on CNGB Sequence Archive (CNSA) of China National Genebank DataBase (CNGBdb) with accession number CNP0006173. The clean reads were aligned to the reference genome of *Cucurbita moschata* (http://cucurbitgenomics.org/). DESeq2 pac kage was applied to analyze the differentially expressed genes (DEGs) between green and yellow stems, including S1 vs. S2, S1 vs. S3, YS1 vs. YS2, and YS1 and YS3. Genes that differently expressed with p-value less than 0.05 after statistical significance testing were considered as significant [17]. Genes were annotated and enrichment analysis were performed using the Gene Ontology (GO), Kyoto Encyclopedia of Genes and Genomes (KEGG), and Nr databases.

GWAS and WGCNA

The factored spectrally transformed linear mixed model (FaST-LMM) (v2.07) was performed for GWAS [18]. The data of single nucleotide polymorphism (SNP) used for the association analysis was from the *Cucurbita moschata* genome (http://cucurbitgenomics.org/). A threshold of -log10(p) = 5 was used for the significant association detection in the study. Genes located within the extended either upstream or downstream 100 kb region of all significant SNPs were considered as candidate genes relevant to the target phenotype. Following, expression data of all potential trait-associated genes was extracted from the above transcriptome data. WGCNA was conducted using the FPKM values of these potential genes [19]. DEGs that could be associated with the chlorisis were discovered by gene annotation and expression changes in different pumpkin varieties.

Quantitative real-time PCR

RNA isolation and cDNA synthesis were performed as previously described [17]. Differentially expressed genes related to the pumpkin stem yellowing were selected for validation. Primers for gene amplification were designed using Primer Premier 5 (Supplementary Table 2). The internal reference gene actin was used to normalize the expression levels. The amplification was conducted on

the CFX96 machine (Bio-Rad, CA, United States). The relative gene expression levels were determined using the $2^{-\Delta\Delta CT}$ method.

Results

Morphology characterization, photosynthetic pigments variation and chloroplast defects of pumpkin yellow stems

The mature stem colors of S1, S2 and S3 were dark green, yellow and pale yellow, respectively (Fig. 1-A-B). However, slightly green color was found in the young yellow stems YS2 and YS3, indicating the de-greening process during the stem development. Interestingly, the greenness of YS2 and YS3 was not comparable to YS1, hinting the absence of pigments since the initial stage of yellow stem development. Physiological analysis found photosynthetic pigments chlorophylls and carotenoids were dramatically reduced (Fig. 1-C-F), which led to the prominent stem chlorisis. In addition, young yellow stems YS2 and YS3 had relatively higher content of pigments than mature stems S2 and S3 (Fig. 1-C and E), which results were consistent with the displayed phenotypes. Another index chlorophyll a/b ratio was decreased with the stem development (Fig. 1-D and F). However, the chlorophyll a/b ratio in S2 and S3 was significantly

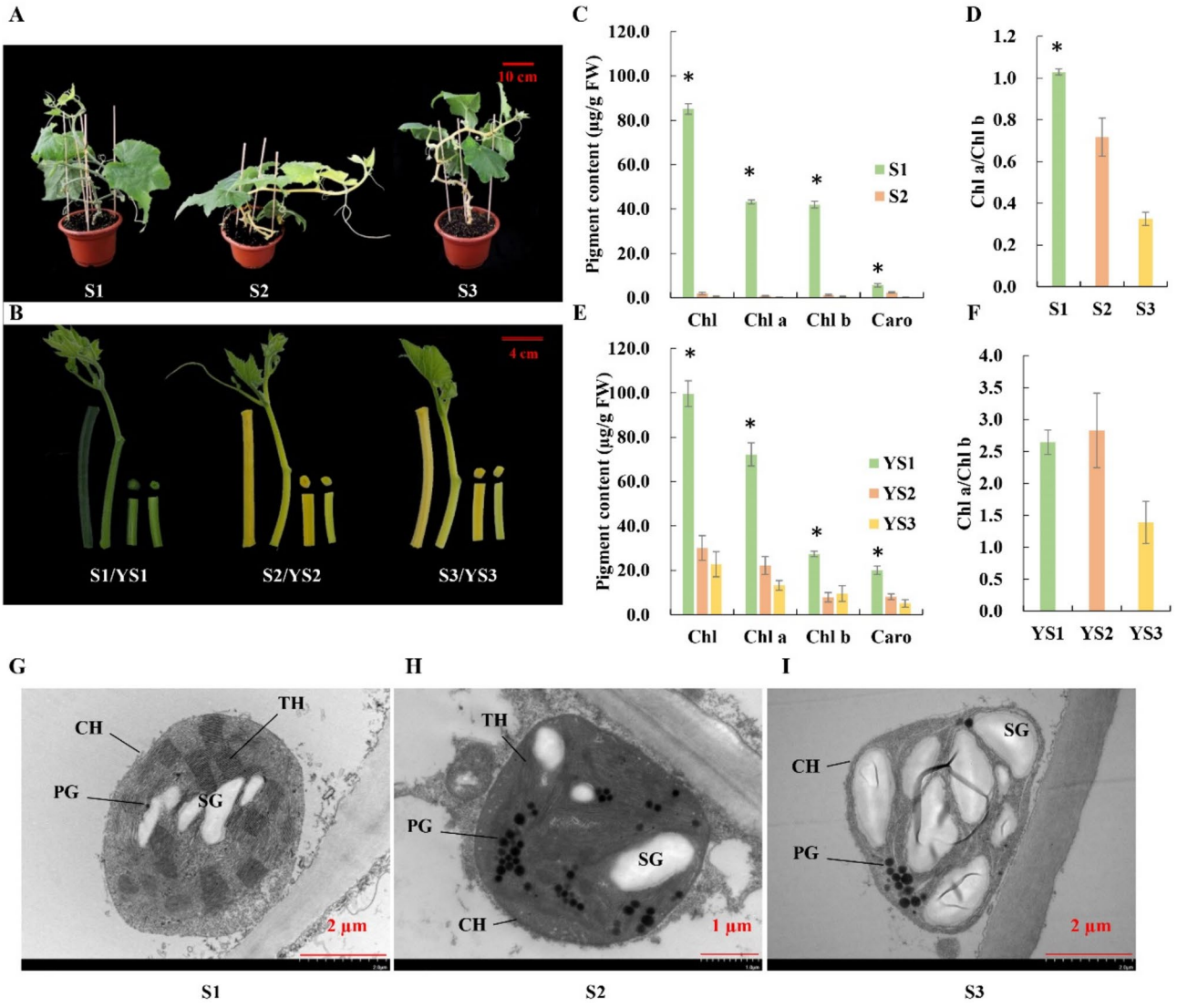

Fig. 1 The phenotypic comparison of three different pumpkin varieties (S1, S2 and S3), and the analysis of photosynthetic pigments and chloroplast ultrastructures of pumpkin stems. (**A**) Three pumpkin varieties S1, S2 and S3. (**B**) The stems of three pumpkin varieties at two different developmental stages (mature stems S1, S2 and S3, young stems YS1, YS2 and YS3), including the whole stem segment, and the corresponding transverse and longitudinal sections. (**C**) Contents of photosynthetic pigments of the pumpkin mature stems. (**D**) Chlorophyll a/b ratio of the pumpkin mature stems; (**E**) Contents of photosynthetic pigments of the pumpkin young stems. (**F**) Chlorophyll a/b ratio of the pumpkin young stems; "* " indicates the significant difference of the same index between green and yellow stems (t-test, $p < 0.05$). **G-I**. Chloroplast ultrastructures of the pumpkin mature stems of S1, S2 and S3 (CH, chloroplast; SG, starch grain; TH, thylakoid; PG, plastoglobule)

lower than S1. And, S3 had the lowest chlorophyll a/b ratio, which may explain the pale yellow stem color.

Notably, no chlorisis was observed in the pumpkin leaf as previously indicated. The finding was consistent with results from the photosynthesis measurements (Supplementary Fig. 1). The relative chlorophyll content in yellow tissues was significantly lower than the green tissues (Supplementary Fig. 1-A). However, the chrolophyll contents in leaves from two pumpkin accessions separately with normal green and yellow stems were similar (Supplementary Fig. 1-B). Interestingly, chlorophyll fluorescence parameters, including ΦPSII, Fv'/Fm' and qP in the pumpkin with yellow stems were all significantly higher (Supplementary Fig. 1-C-H). Further, examination of stem sections through transmission electron microscopy found few difference in the chloroplast number in the cell from three stem materials. However, abnormal chloroplast ultrastructure with disrupted thylakoid systems were discovered in both S2 and S3, together with the accumulated plastoglobules and presented starch grains (Fig. 1-G-I). The increased plastoglobules size in yellow stems could be correlated with the disassembly of the thylakoid system. However, S1 had intact chloroplast structure.

Gene expression profiles and enrichment analysis

The pumpkin stem transcriptome analysis identified 31,470 genes, including 1135 novel genes (Supplementary Table 3). Comparative analysis was performed to discover DEGs in yellow stems (Supplementary Fig. 2). There were 8175 (S2 vs. S1, 4550 up-regulated, 3625 down-regulated) (Supplementary Table 4), 6957 (S3 vs. S1, 3777 up-regulated, 3180 down-regulated) (Supplementary Table 5), 5031 (YS2 vs. YS1, 2887 up-regulated, 2144 down-regulated) (Supplementary Table 6), and 4537 (YS3 vs. YS1, 2328 up-regulated, 2209 down-regulated) (Supplementary Table 7) DEGs found, respectively. Genes with increased expression were more than those with decreased abundance in the specific comparions between the yellow and green stems. It was apparent that more DEGs (62.5% increase in S2-vs-S1 than YS2-vs-YS1, 53.3% increase in S3-vs-S1 than YS3-vs-YS1) were induced in mature yellow stems, indicating more genes were involved in the process of stem yellowing. Upset analysis identified 641 significantly regulated genes in four different comparisons (S2 vs. S1, S3 vs. S1, YS2 vs. YS1, and YS3 vs. YS1) (Supplementary Fig. 2-B, Supplementary Table 8).

GO functional classification were applied to clarify the molecular function of DEGs in yellow stems. The top ten functional categories were displayed (Fig. 2-A-D). With the stem development, expression of genes related to cytoskeletal protein binding, microtubule binding, and tubulin binding were prominently decreased in mature yellow stems. Kinesin, myosin, and microtubule-associated protein that with the function of cytoskeletal protein binding were found and down-regulated. In addition, GO analysis were separately applied to DEGs with increased and decreased expression. Biological processes photosynthesis and chloroplast organization were enriched and mostly up-regulated, whereas phosphorylation, cell cycle, and cell division related genes were down-regulated in yellow stems (Fig. 2-E, Supplementary Fig. 3–4). Besides, KEGG analysis identified regulated carbon metabolism (S2 vs. S1 and S3 vs. S1), biosynthesis of secondary metabolites (S2 vs. S1, S3 vs. S1, YS2 vs. YS1, and YS3 vs. YS1), biosynthesis of amino acids (S2 vs. S1, S3 vs. S1, and YS2 vs. YS1), phenylpropanoid biosynthesis (YS2 vs. YS1 and YS3 vs. YS1), and alanine, aspartate and glutamate metabolism (S2 vs. S1 and S3 vs. S1) (Fig. 2-F, Supplementary Fig. 5–8). Further STRING analysis found 67 of the 641 common DEGs were enriched in five biological processes, including response to light stimulus, photosynthesis, thylakoid membrane organization, chloroplast organization, and plastid organization. Expression analysis found most genes in these biological processes were up-regulated in yellow stems (Supplementary Fig. 9).

Abnormal metabolism and accumulation of chlorophylls and carotenoids

The metabolism of chlorophylls and carotenoids in yellow stems was analyzed because of the identification of abnormal pigment accumulation. Porphyrin is vital to the production of chlorophylls. DEGs in S2 and S3 were enriched in porphyrin metabolism, which could be important during the stem coloring (Fig. 3, Supplementary Tables 4, 5, 6, 7). Protochlorophyllide reductase (POR) and chlorophyllide a oxygenase (DVR) coding genes were regulated and all significantly increased in either mature or young yellow stems of S2 and S3, indicating the increased formation of chlorophyllide a. However, chlorophyllase (*CLH*), pheophorbide a oxygenase (*PAO*) and red catabolite reductase (*RCCR*) were all increased in S2 and S3. These genes play important roles in chlorophyll degradation. The higher abundance of chlorophyll(ide) b reductase (*NOL*) and 7-hydroxymethyl chlorophyll a reductase (*HCAR*) coding genes were also found in yellow stems. They are essential during the conversion of chlorophyll b to chlorophyll a. The up-regulated genes involved in the chlorophyll degradation could be related to the few chlorophylls found in yellow stems.

DEGs involved in carotenoid biosynthesis and metabolism were also analyzed. *PSY*, *PDS*, *Z-ISO*, *ZDS*, *CRTISO*, *LCYE* and *LCYB* involved in carotene biosynthesis, *LUT1*, *CRTZ*, and *LUT5* involved in lutein biosynthesis, *DWARF27*, *CCD7* and *CCD8* involved in carlactone biosynthesis, *VDE*, *ZEP*, *NXS*, *NCED*, *ABA2* and *AAO3* involved in ABA biosynthesis, were mostly up-regulated

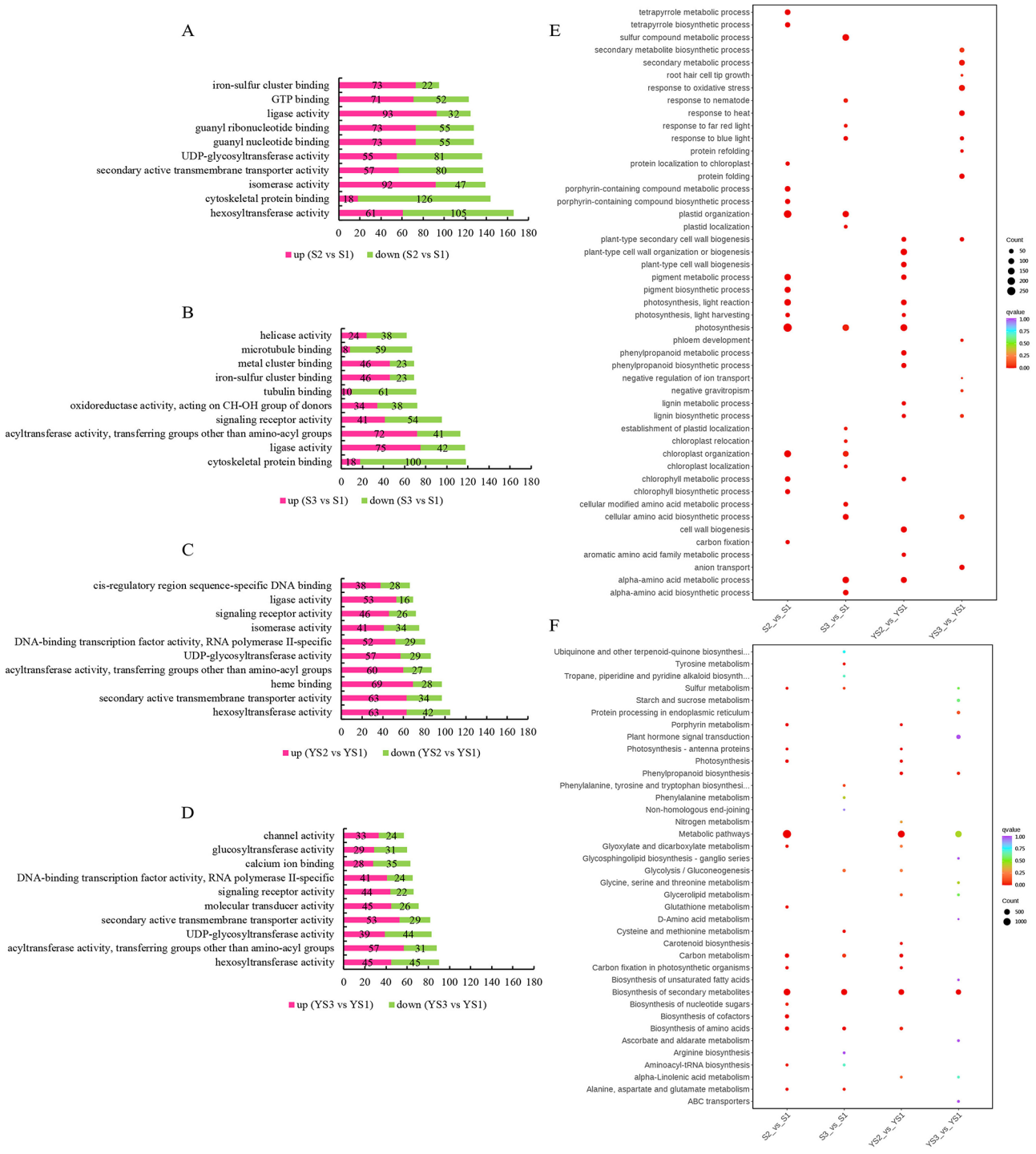

Fig. 2 GO and KEGG analysis. **A**-**D**. Top ten enriched GO functional categories using DEGs in yellow stems (**A**. S2 vs. S1, **B**. S3 vs. S1, **C**. YS2 vs. YS1, **D**. YS3 vs. YS2) (ranked according to the percentage of DEGs annotated on the specific GO category to all DEGs). The purple and green colors separately represent the number of up- and down-regulated genes. **E**-**F**. The combined enrichment analysis of DEGs from four different comparisons. The upper (**E**) and lower (**F**) bubble charts separately showed the GO and KEGG enrichment results. The q value of all enriched pathways in the specific comparison was ranked, and the top 15 pathways with the lowest q value from four comparisons were combined and displayed. The y-axis and x-axis separately represent the enriched pathways in the corresponding comparisons. The bubble size and color separately represent the number of DEGs enriched in the corresponding pathways and the enrichment significance

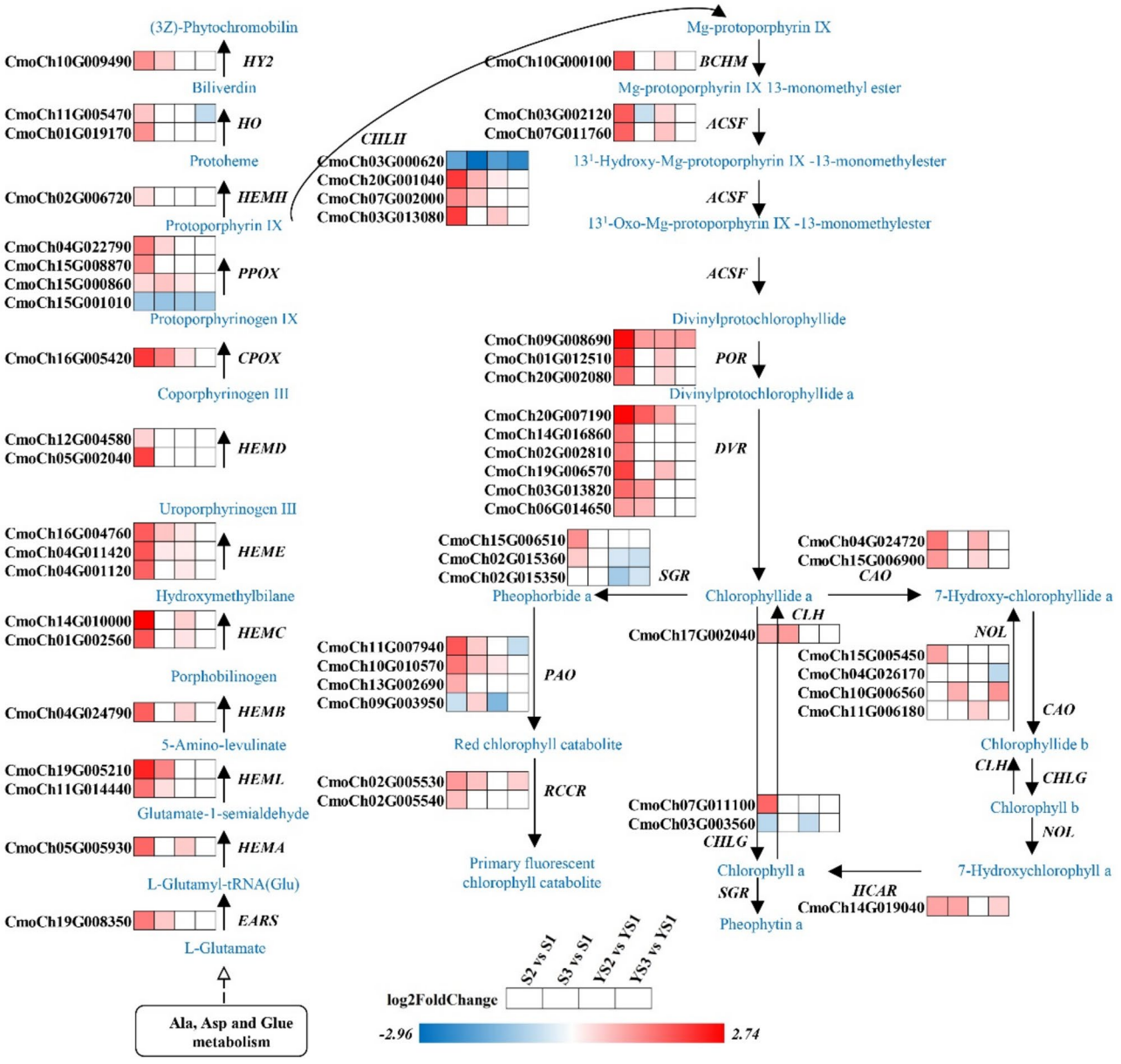

Fig. 3 Heatmaps of DEGs related to KEGG pathway porphyrin metabolism. *EARS*, glutamyl-tRNA synthetase; *HEMA*, glutamyl-tRNA reductase; *HEML*, glutamate-1-semialdehyde 2,1-aminomutase; *HEMB*, porphobilinogen synthase; *HEMC*, hydroxymethylbilane synthase; *HEME*, uroporphyrinogen decarboxylase; *HEMD*, uroporphyrinogen-III synthase; *CPOX*, coproporphyrinogen III oxidase; *PPOX*, protoporphyrinogen/coproporphyrinogen III oxidase; *HEMH*, protoporphyrin/ coproporphyrin ferrochelatase; *HO*, heme oxygenase; *HY2*, phytochromobilin: ferredoxin oxidoreductase; *CHLH*, magnesium chelatase subunit H; *BCHM*, magnesium-protoporphyrin O-methyltransferase; *ACSF*, magnesium-protoporphyrin IX monomethyl ester (oxidative) cyclase; *POR*, protochlorophyllide reductase; *DVR*, chlorophyllide a oxygenase; *SGR*, magnesium dechelatase; *PAO*, pheophorbide a oxygenase; *RCCR*, red chlorophyll catabolite reductase; *CLH*, chlorophyllase; *CHLG*, chlorophyll/bacteriochlorophyll a synthase; *CAO*, divinyl chlorophyllide a 8-vinyl-reductase; *NOL*, chlorophyll(ide) b reductase; *HCAR*, 7-hydroxymethyl chlorophyll a reductase. Red and blue colors separately represent the increase and decrease in the abundance of genes in corresponding comparisons

in yellow stems (Fig. 4, Supplementary Tables 4, 5, 6, 7). In detail, *six PSY genes*, *encoding* the major rate-limiting enzyme in carotenoid biosynthesis, were significantly regulated. And, five *PSYs* were increased in either S2 or S3. In addition, *PDS* and *CRTISO*, which of catelyzation result in the generation of lycopene, were all with increased expression in yellow stems. Following, *LYCE* and *LYCB* that contribute to the formation of carotene, increased in S2, in particular. *ZEP* and *VDE* which are vital to the epoxidation and de-epoxidation of zeaxanthin to form antheraxanthin and violaxanthin in the core carotenoid biosynthetic pathway, were elevated in young yellow stems. Concurrently, up-regulated *CCD7*, *CCD8* and *DWARF27* in carlactone biosynthesis implied the

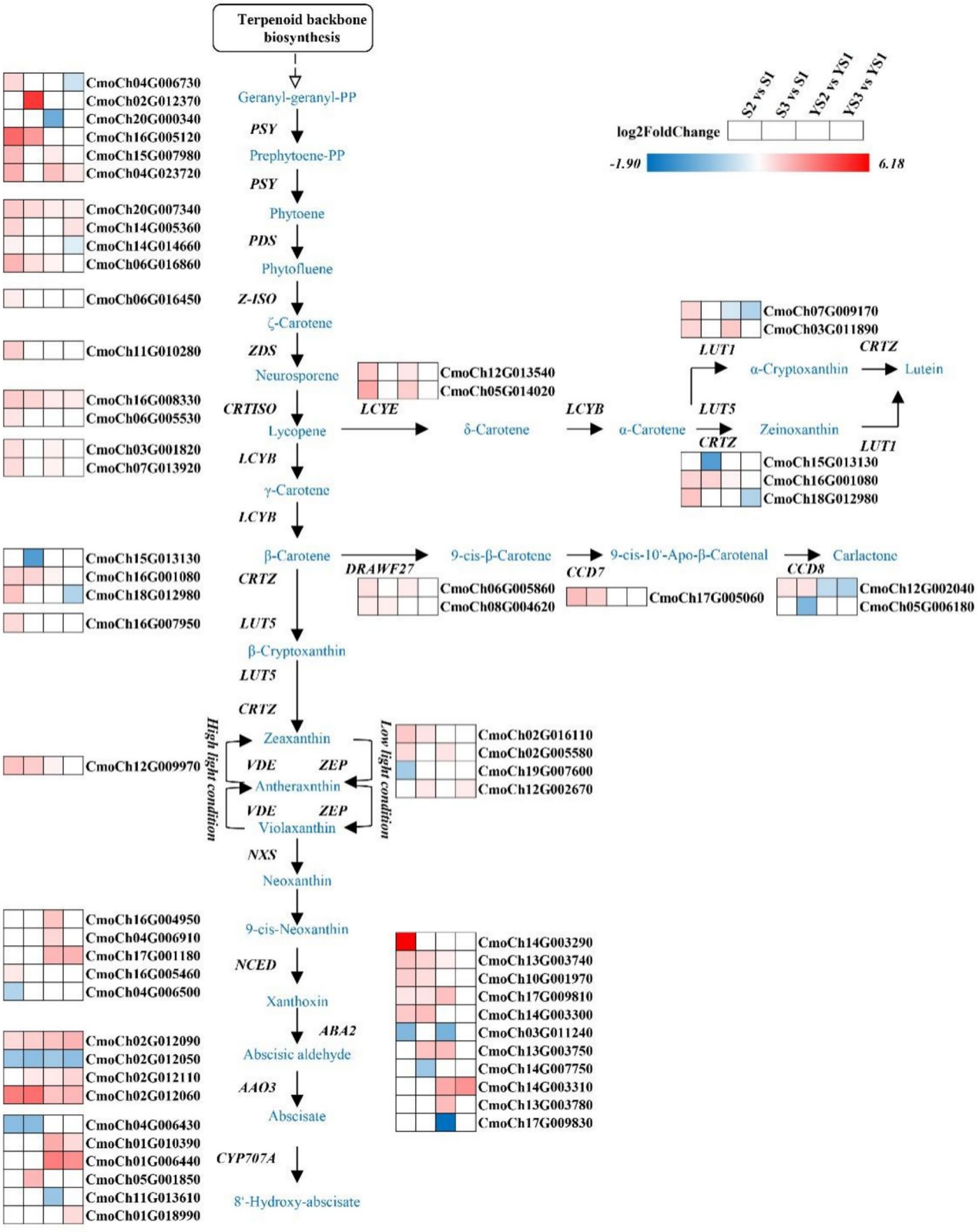

Fig. 4 (See legend on next page.)

(See figure on previous page.)

Fig. 4 Heatmaps of DEGs involved in KEGG pathway carotenoid biosynthesis and metabolism. *PSY*, 15-cis-phytoene synthase; *PDS*, 15-cis-phytoene desaturase; *Z-ISO*, zeta-carotene isomerase; *ZDS*, zeta-carotene desaturase; *CRTISO*, prolycopene isomerase; *LCYE*, lycopene epsilon-cyclase; *LCYB*, lycopene beta-cyclase; *LUT1*, carotenoid epsilon hydroxylase; *CRTZ*, beta-carotene 3-hydroxylase; *LUT5*, beta-ring hydroxylase; *DWARF27*, beta-carotene isomerase; *CCD7*, 9-cis-beta-carotene 9',10'-cleaving dioxygenase; *CCD8*, carlactone synthase/all-trans-10'-apo-beta-carotenal 13,14-cleaving dioxygenase; *VDE*, violaxanthin de-epoxidase; *ZEP*, zeaxanthin epoxidase; NXS, neoxanthin synthase; *NCED*, 9-cis-epoxycarotenoid dioxygenase; *ABA2*, xanthoxin dehydrogenase; *AAO3*, abscisic-aldehyde oxidase; *CYP707A*, (+)-abscisic acid 8'-hydroxylase. Red and blue colors represent increased and decreased expression of genes in corresponding comparisons, respectively

enhanced carotenoid catabolism in mature yellow stems. Additionally, 11 *ABA2* and four *AAO3* genes in ABA biosynthesis pathway were regulated and mostly increased in yellow stems, implying the enhanced ABA production.

Increased expression of thylakoid membrane constituents, chloroplast development-associated factors, and plastoglobule proteins coding genes

Extensive regulations on constituents of thylakoid membranes were identified in yellow stems, including 31 genes belonging to LHC, 41 genes in PSII, 20 genes in PSI, 12 genes mediating the photosynthetic electron transport, and 18 genes encoding the F-type ATPase subunits (Fig. 5, Supplementary Tables 4, 5, 6, 7). These DEGs were enriched in KEGG pathways photosynthesis and photosynthesis-antenna proteins. Most of them were up-regulated in yellow stems, especially in S2, indicating efforts to improve the photosynthetic reactions.

Genes related to the chloroplast development were analyzed. The fluctuant expression of a large number of *PPRs* was identified. There were separately 59, 39, 22 and 25 *PPRs* regulated in four comparisons S2 vs. S1, S3 vs. S1, YS2 vs. YS1, and YS3 vs. YS1 (Supplementary Tables 4, 5, 6, 7). Interestingly, most *PPRs* were increased in yellow stems. There were 42 (71.2% of the regulated) and 28 (71.8% of the regulated) *PPRs* had increased expression in S2 and S3, respectively. Similarly, the abundance of 12 and 22 *PPRs* were separately increased in YS2 and YS3. Further analysis found most *FtsH* had higher expression in yellow stems. All regulated *FtsH* (17 in S2, eight in S3, and five in YS2) displayed increased expression in yellow stems. Only one *FtsH* had decreased abundance in YS3 (three up-regulated, one down-regulated). In addition, the regulation of *mTERF* was also discovered in yellow stems. A total of 13 (10 increased, three decreased), 10 (six increased, four decreased), eight (four increased, four decreased), and seven (four increased, three decreased) *mTERFs* were regulated in S2, S3, YS2 and YS3, respectively. Therefore, chloroplast development associated genes were mostly increased. It is likely that the chloroplast defects was controlled by other factors.

Following, transcriptome analysis found genes encoding the distinct proteome of chloroplast plastoglobules, including four BC1 (ABC1 complex) kinases, one tocopherol cyclase (*VTE1*), and four carotenoid cleavage dioxygenase (*CCD4*). The abundance of four *ABC1K3* (*CmoCh02G002390*, *CmoCh03G008080*, *CmoCh05G006600* and *CmoCh11G012660*) were all higher in S2 than S1. These *ABC1K3* had comparable abundance among young stems. Except for *CmoCh03G008080*, the expression of other three *ABC1K3* increased with stem maturation. The expression changes of *ABC1K3* could be associated with the increased plastoglobules in the chloroplast. However, neither *VET1* nor *CCD4* had apparent expression changes among three varieties.

Up-regulation of ribosome and proteasome KEGG pathways

Notably, enrichment analysis identified 190 DEGs enriched in the KEGG pathway ribosome, including 110 large and 80 small ribosomal subunit coding genes. A big portion of these genes had higher expression in young stems than mature stems, which is in line with the necessity of plant development (Fig. 6-A, Supplementary Tables 4, 5, 6, 7). GO annotation found 73 chloroplast ribosomal subunits, including 34 genes encoding the 50 S large ribosomal subunits and 13 genes encoding the 30 S small ribosomal subunits. The 50 S and 30 S ribosomal subunits belong to the 70 S ribosome which is involved in protein biosynthesis in chloroplasts. Gene expression analysis revealed that these chloroplast ribosome genes were mostly increased in mature yellow stems S2 and S3 (Fig. 6-B, Supplementary Tables 9, 10, 11), which was consistent with the overall increase of the chloroplast protein coding genes. Strikingly, more fluctuations of ribosome associated genes were identified in S2, suggesting the vigorous protein biosynthesis in the pumpkin variety S2.

Similarly, up-regulated KEGG pathway proteasome was found in yellow stems, especially in S2 (Fig. 6-C). There were 40 DEGs, including 20 genes encoding the 20 S proteasome subunits, 16 genes encoding 26 S proteasome regulatory subunits, one proteasome activator subunit 4, one proteasome inhibitor subunit 1 (PI31), one 26 proteasome complex subunit DSS1, and one proteasome maturation protein. Three proteasome subunits *CmoCh14G012210* (20 S proteasome subunit alpha 1), *CmoCh06G013990* (20 S proteasome subunit beta 4), *CmoCh12G006140* (26 proteasome complex subunit DSS1) were up-regulated in the mature yellow stems S2 and S3.

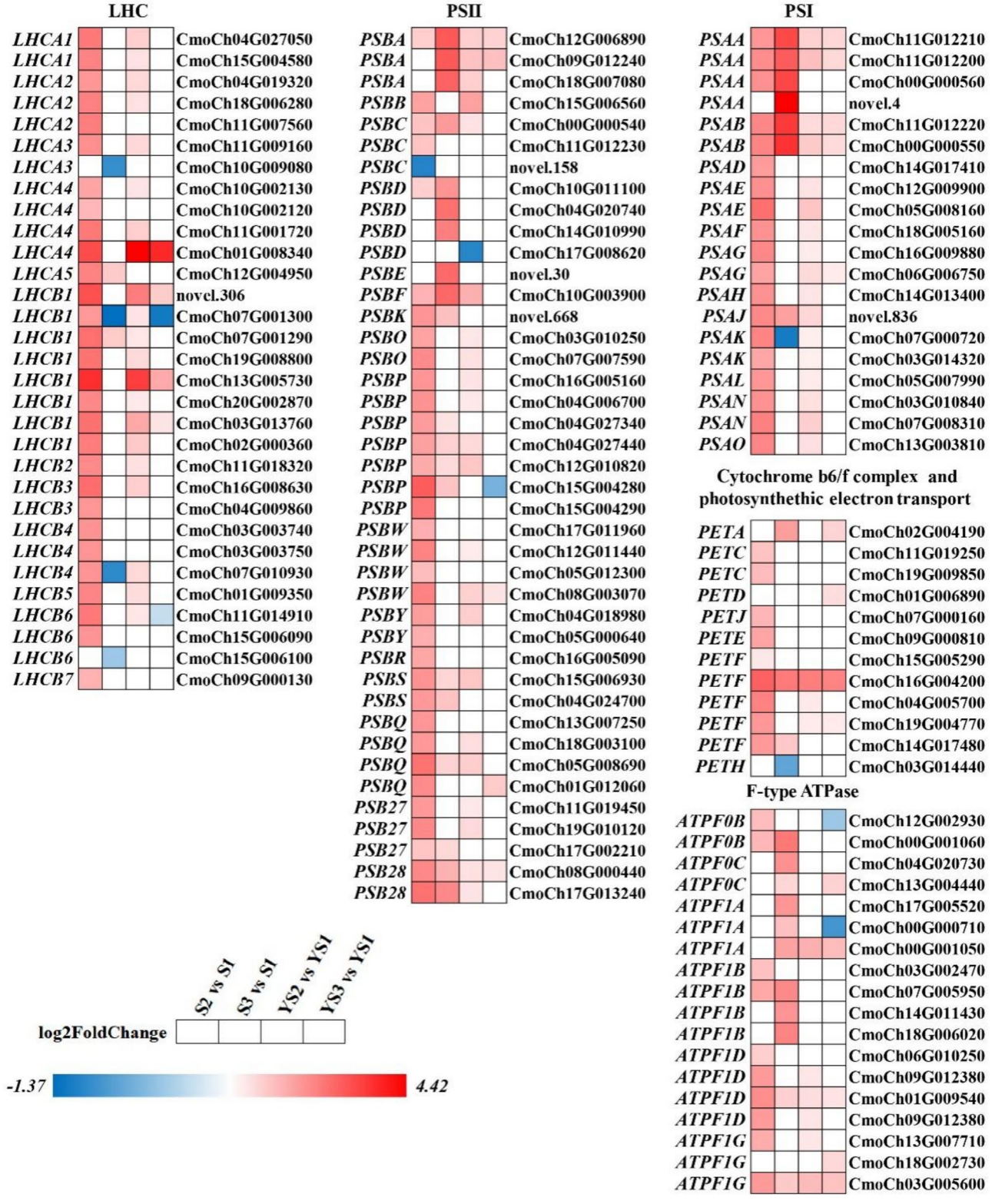

Fig. 5 Heatmaps of DEGs involved in photosynthesis. LHC, light harvesting chlorophyll protein complex; PSI, photosystem I; PSII, photosystem II. Red and blue colors separately represent the up- and down-regulation of genes in corresponding comparisons

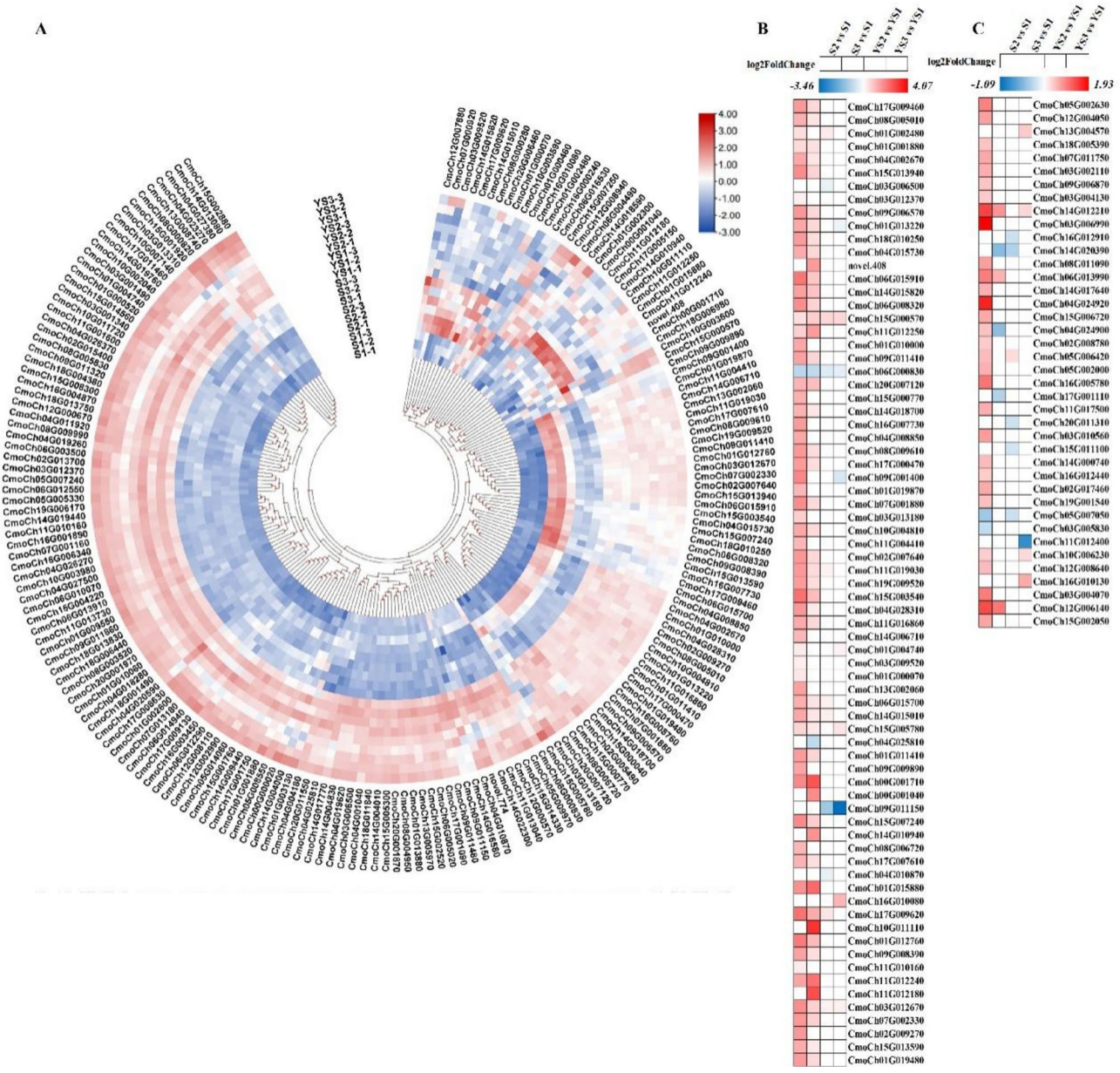

Fig. 6 Heatmaps of DEGs involved in KEGG pathways ribosome and proteasome, respectively. (**A**) DEGs involved in pathway ribosome. (**B**) DEGs belonging to chloroplast ribosome. (**C**) DGEs involved in pathway proteasome. Red and blue colors separately represent the increase and decrease in the abundance of genes in the correspnding comparisons

GWAS and integrated analysis with transcriptome

There were 104 trait-related single-nucleotide polymorphisms (SNPs) identified, with the prominent SNPs being discovered on chromosome 14. 906 genes were located within the extended regions of all significant SNPs (Fig. 7-A, Supplementary Table 1). 129 out of the 906 genes had SNP either on the coding sequence or the corresponding promoter (upstream 3000 bp of the initiation codon). GO analysis found that 92 genes belonged to the cellular component chloroplast, and part of them were involved in photosynthesis. The integrated GWAS and transcriptome data found the up-regulated chloroplast components in yellow stems (Fig. 7-B). WGCNA analysis using the expression data of the GWAS-identified genes generated four modules (Supplementary Tables 12, 13, 14, 15, Supplementary Fig. 10-A-D). Genes in the blue module had higher expression in yellow stems, and a big portion of them were associated with chloroplast or photosynthesis (Supplementary Table 12). The top hub gene in the blue module was *CmoCh20G008280* (Cathepsin B-like cysteine proteinase). In addition, the abundance of *CmoCh20G008280* in mature stems was higher than

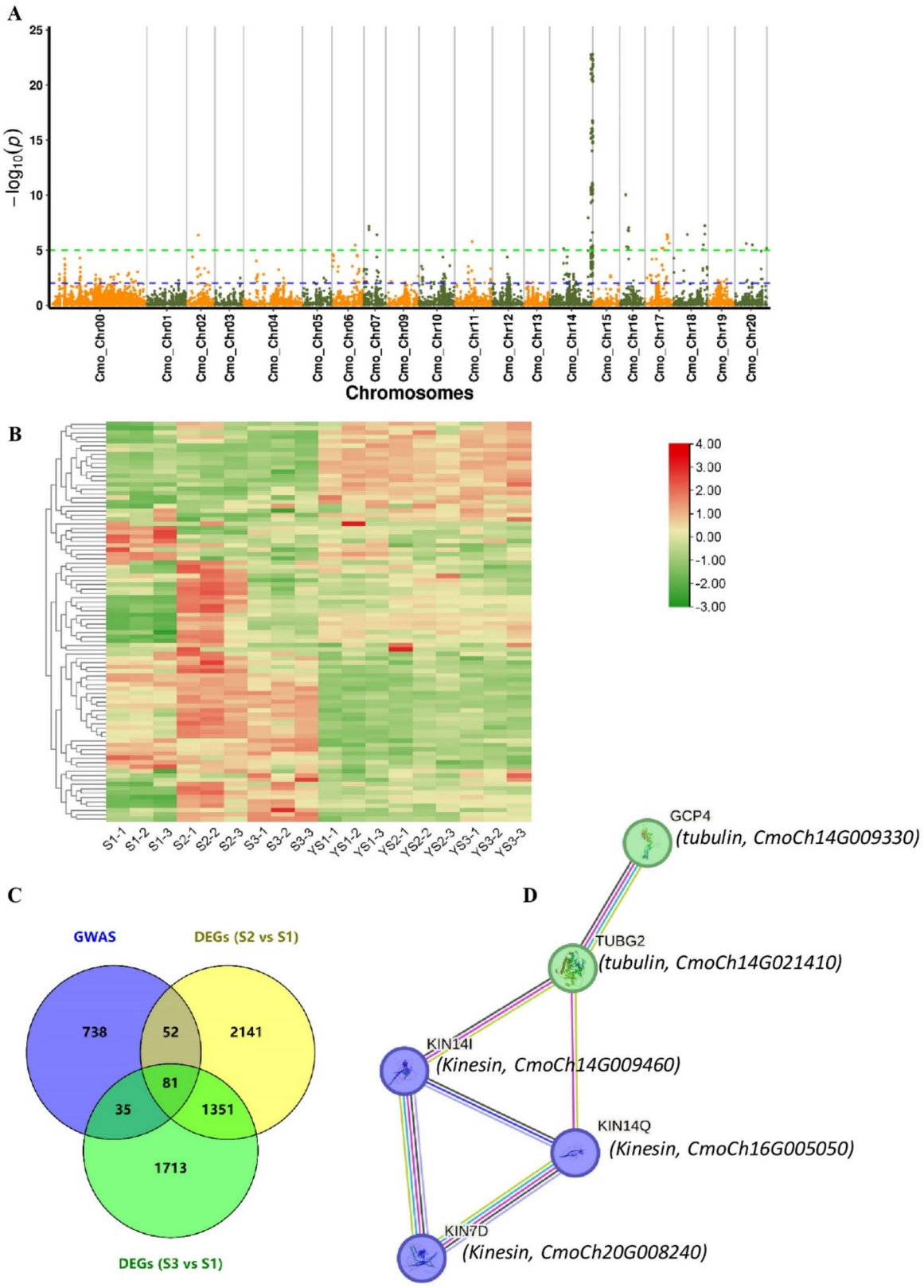

Fig. 7 GWAS and gene expression analysis related to stem colors. (**A**) Manhattan plot generated from GWAS results by FaST-LMM. The y-axis and x-axis separately represent the $-\log_{10}(p)$ and chromosome locations. A threshold of $-\log_{10}(p) = 5$ was used for the significant association detection. (**B**) Heatmap generated using the FPKM of 92 genes that belong to the cellular component chloroplast. (**C**) Venny analysis of the GWAS identified genes, and DEGs in yellow stems S2 and S3. (**D**) Kinesin and tubulin coding genes enriched in the microtubule-based biological process

young stems, indicating the potential function during stem development and yellowing. Genes in turquoise (Supplementary Table 13) and yellow modules (Supplementary Table 14) had the pattern of lower expression in yellow stems. 81 genes identified by GWAS were down-regulated in both S2 and S3 (Fig. 7-C).

String analysis of these genes found five regulated genes enriched in microtubule-based biological process (Fig. 7-D), including three kinesin coding genes (*CmoCh16G005050*, *CmoCh14G009460* and *CmoCh20G008240*), and two tubulin coding genes (*CmoCh14G009330* and *CmoCh14G021410*). It is notable that *CmoCh14G009460* (position: 5027092 ~ 5033298, number of exons: 18 exons) was located on chromosome 14 and was the only one of the five genes that had SNP (C/T, position: 5034400, *p* value = 7.41E-06) detected on the promoter (ATG start codon upstream 565 bp). *CmoCh14G009460* is the homolog of *Arabidopsis thaliana* kinesin-14 member *KIN14I*. The expression of *CmoCh14G009460 in* yellow stems were just half of that in green stems. In addition, it has the highest expression compared to other two *kinesin* genes. These findings suggested that *CmoCh14G009460* could be one of the candidate genes associated with the stem yellowing. The promoter analysis of *CmoCh14G009460* using PlantPAN found the change of C to T resulted the loss of transcription factor (TF) binding sites, including bZIP, NAC, AP2, Trihelix and bHLH TFs. There were 1080 differentially expressed TFs. And 38 TFs were regulated in all four comparisons, indicating the potential roles during stem yellowing (Supplementary Fig. 11).

qRT-PCR validation

Genes with distinct expression profiles between the yellow and green stems were selected for qRT-PCR validation (Supplementary Table 2). The expression patterns of these genes determined by qRT-PCR was highly consistent with RNA-seq data, which indicated that the reliability of the transcriptome data (Supplementary Fig. 12).

Discussion

Similar yet different mechanisms were involved in the pumpkin stem coloring

Mounting evidence has proven variations in chloroplast development, photosynthetic pigments metabolism, and photosynthesis during the coloring of plant tissues [5, 7, 20]. However, thees processes could be controlled by various factors, resulting in species-specific color changes. There were a considerable number of reports on abnormal yellowing, albinism or leaf senescence with varied phenotypes [21, 22]. However, few studies demonstrated the molecular mechanisms underlying the pumpkin stem coloring. The abnormal accumulation of photosynthetic pigments and disrupted thylakoid membrane found in pumpkin stems were also discovered in rice yellow leaves [23] and Ginkgo striped white leaves [24]. However, the accumulated plastoglobules in mature yellow stems, along with the presence of starch grains, were different from the previous findings [5, 7]. Plastoglobules have function in lipid biosynthesis and act as the storage site for thylakoid membrane catabolites. They become supersized after the chlorophyll degradation [25–27]. It is notable that leaf of the pumpkin varieties with yellow stems were normal and green, whereas, pumpkin stem yellowing happened at the early stage of its development and aggravated with the maturation. Hence, the pumpkin stem yellowing was tissue-specific and could be impacted by the plant development. It was suggested that similar yet different genetic factors could be involved in the pumpkin stem yellowing.

Abnormal metablism of photosynthetic pigments were associated with the stem yellowing

The failed pigment accumulation in pumpkin yellowing stems suggested there could be abnormal pigment catabolism. Previously, expression of chlorophyll biosynthesis genes (*POR* and *DVR*) decreased and chlorophyll degradation gene (*SGR*) increased in jujube albino leaves [5]. In similar, up-regulated chlorophyll degradation genes (*NOL*, *HCAR*, *CLH*, *PAO* and *RCCR*) were found in yellow stems. *CLH* is the rate-limiting enzyme in chlorophyll catabolism. It was reported that expression of *Citrus sinensis CLH* led to extensive chlorophyll breakdown in both tobacco protoplasts and squash leaves [28]. *NOL* and *HCAR* are important genes during the conversion of chlorophyll b to chlorophyll a, while down-regulation of them could block the process. It was reported that PAO cleaves the porphyrin ring of the chlorophyll catabolites and results in the loss of green color [29]. The synchronous increase of these genes could significantly diminish chlorophylls, leading to stem de-greening.

In addition to chlorophylls, the regular synthesis and degradation of carotenoids are also crucial in green tissues. *PSY* plays a critical role in controlling the total amount of synthesized carotenoids. In the study, the massive up-regulation of *PSYs* indicated the accelerated condensation of GGPP (geranyl-geranyl-PP) which is a precursor for chlorophyll and gibberellin biosynthesis [4, 30]. β-carotene and lutein, together with violaxanthin and neoxanthin, are the richest carotenoids in the chloroplast. Genes involved in the biosynthesis of β-carotene and lutein was enhanced in yellow stems. It is inconsistent with the decreased expression of genes involved in the carotenoid biosynthesis in the arecanut and tea with leaf albinism [7, 31]. *ZEP* and *VDE*, which are vital for the generation of violaxanthin and neoxanthin, were increased in yellow stems, and could be helpful in the protection of plants from photo-oxidative damage (Jahns

and Holzwarth, 2012). *CCD* and *NCED* are responsible for the oxidative cleavage of carotenoids and were up-regulated in yellow stems. Increased *CmCCD4a* transcript levels lead to the degradation of yellow carotenoid pigments, resulting in the loss of greenness and white petals in chrysanthemum [32]. *CCD7* and *CCD8* act together for the biosynthesis of carlactone which is the ultimate biosynthetic precursor of all naturally occurring strigolactones [33]. It is reported that *NCED2*, *3*, *5*, *6*, *9* are involved in ABA production [34]. *NCEDs* were most up-regulated in young yellow stems. In addition, 11 *ABA2* and four *AAO3* genes involved in the ABA biosynthesis were mostly up-regulated in mature yellow stems. Plants could generate higher ABA under unfavorable conditions, which reduces photosynthetic capacity by inhibiting the thylakoid formation, rubisco activity, and chlorophyll biosynthesis [14, 15].

Compensate mechanisms were activated to respond to the chloroplast defects

Strikingly, comparative transcriptome analysis between yellow and green stems at the same developmental stages found that more genes were regulated in mature yellow stems. For instance, four regulated chloroplast plastoglobule-localized Abc1 kinases were all increased in S2. Abc1 kinases are involved in plastoglobule prenyllipid metabolism [35]. They are important for photo-oxidative stress tolerance and chloroplast morphology. Loss of ABC1K1 and ABC1K3 led to conditional chlorisis of *Arabidopsis thaliana* [36]. In addition, chloroplast development associated genes *PPRs*, *FtsH* and *mTERF* were triggered and up-regulated in yellow stems.

Photosynthetic pigments are mostly associated with protein components of photosystems that reside in thylakoids. The disrupted accumulation of photosynthetic pigments could be followed by decreased photosynthesis and abnormal plant development [7]. Unexpectedly, the up-regulated pigment metabolism and photosynthesis were concurrently found in yellow stems. Genes related to LHC, PSI, PSII, photosynthetic electron transport and ATPase were up-regulated, especially in S2, indicating enhanced photosynthetic reactions. The regulation could be the response of yellow stems to the impaired thylakoid system. It was reported that the chlorophyll reduction in rice *ygl* did not affect the expression of light capture antenna complex and light capture chlorophyll binding proteins [37]. The similar regulatory mechanism was found in mature leaves of *Ziziphus jujuba* Mill. that displayed albino phenotype [5].

Except for these mechanisms, robust up-regulation of peroxidase coding genes was identified in yellow stems, and the expression of all regulated peroxidase increased with the stem development, which may mediate the degradation of chlorophyll and its derivatives [38]. The up-regulated genes in these pathways, together with the ribosome pathway which is well-known for gene translation, could be activated to maintain the development of pumpkin yellow stems. The compensation mechanisms were also reported in albino leaves of the jujube and arecanut [5, 7].

It is notable that genes involved in porphyrin metabolism, carotenoid biosynthesis and metabolism, photosynthesis, carbon fixation and ribosome were mostly up-regulated in S2, indicating the diverse regulation on stem coloring. Higher expression of genes related to photosynthesis, and biosynthesis and metabolism of photosynthetic pigments were more evident in S2 when compared to its corresponding young stems YS1 (Supplementary Tables 9, 10, 11). These results indicated there were more fluctuations induced with the development of yellow stems. Those mechanisms may cooperate mutually and play important roles in maintaining stem development, which makes S2 an ideal material for the further study of chloroplast development, photosynthesis, and associated molecular breeding.

Multiple factors may result in chloroplast defects

Maintenance of photosynthetic apparatus requires the action of proteases [39]. Photosynthesis proteins are ubiquitinated and processed by 26 S proteasome via chloroplast-associated protein degradation (CHLORAD) [40–42]. The 26 S proteasome ubiquitin receptor DSS1 coding gene *CmoCh12G00614* was up-regulated more than two folds in mature yello stems. *CmoCh20G008280*, belonging to the papain family cysteine proteases, could be another candidate involved in the stem yellowing. The papain family cysteine protease could display tissue-specific expression patterns and have great importance in the plant protein degradation [39, 43, 44]. *CmoCh20G008280* displayed increased expression in both young and mature yellow stems. Interestingly, *CmoCh20G008280* was highly expressed in mature stems. Its expression in mature stems S1, S2 and S3 were three to five folds of that in the corresponding young stems. Cysteine protease HvPAP14 was reported to play a role in the chloroplast protein degradation in the barley [45]. HvPAP14 was accumulated in the chloroplast with leaf senescence. It was tightly associated with the thylakoid membrane. The overexpression of *HvPAP14* could degrade bulk chloroplast proteins. Increased papain-like cysteine protease inhibitor *(BoCPI-1)* of broccoli *(Brassica oleracea var. italica)* resulted in down-regulated cysteine protease, and delayed the chlorophyll loss after harvest [46]. The integration of GWAS and transcriptome data identified another trait related candidate gene *CmoCh14G009460* that is the homolog of *Arabidopsis thaliana* kinesin-14. Kinesins are microtubule-based motors, and deliver organelles, vesicles and newly synthesized proteins to intracellular destinations

[47]. They could be essential for chloroplast to move and attach to the plasma membrane. It was reported that kinesin-like protein kac1 mutant of *Arabidopsis thaliana* displayed severely impaired chloroplast accumulation and slow avoidance movement [48]. The double mutant of kac1kac2 lost chloroplast photorelocation movement and presented detached chloroplasts from the plasma membrane [49]. YD1 is the rice kinesin-4 protein, and involved in chlorophyll synthesis and chloroplast development in leaves. The yd1 mutant had severely reduced chlorophyll and disrupted thylakoid ultrastructure, resulting in leaves yellowing and dwarf phenotype [50]. Interestingly, phosphorylation might affect the affinity for different kinesin partners or their redistribution in chloroplast movement machinery [51]. Cyclin-dependent kinase, involved in cell cycle progression, was one of the major kinases that could phosphorylate kinesin proteins [52]. In addition, the phosphorylation sites of kinesin protein were more in the light compared to the darkness. The decreased kinesin and down-regulated phosphorylation biological process may play some role in the chloroplast biology of the yellow pumpkin stems, and their function could be explored in the further.

Additionally, transcriptional regulation could be involved in the stem yellowing process. For instance, transcriptional regulation of cysteine proteases is determined by the cis-acting elements located in the promoters. The expression of related transcription factors (TFs), and the interactions between different TFs could result in diverse spatial and temporal patterns expression of the target gene [53]. BdGAMYB and BdDOF24 were the activators of BdCathB (Cathepsin B-like protease) in *Brachypodium distachyon* [54]. Expression of Kinesin 1 was significantly increased in transgenic *Arabidopsis* plants of peanut AhMYB30 [55], ginseng PgMYB4 [56], and Zea mays MYC-type ICE-like ZmmICE1 transcription factor [57]. However, the function and promoter sequence analysis of the candidate gene, expression analysis of TFs, and the confirmation of interactions are required to understand the regulatory mechanisms in pumpkin yellow stems.

Conclusions

The physiological and cytological analysis were applied to characterise the pumpkin yellow stem phenotype. In addition, transcriptome and GWAS analysis were integrated to discover the underlying molecular mechanisms related to stem coloring. Chloroplast defects and photosynthetic pigment loss led to the pumpkin stem yellowing, which was similar to the previous findings in other plants. The abnormal catabolism could result in the disrupted accumulation of chlorophylls and carotenoids in yellow stems. However, up-regulated genes involved in chloroplast development, photosynthesis, and ribosome indicated that compensatory mechanisms may be triggered to respond to the disruption of thylakoid membrane systems. Multiple factors, for instance, increased proteases and decreased kinesins may contribute to the de-greening process. Chloroplast proteins could be abnormally degraded, and the thylakoid membranes were disrupted. However, further analysis is required to better understand the regulatory mechanisms associated with stem coloring.

Supplementary Information

The online version contains supplementary material available at https://doi.org/10.1186/s12870-025-06673-w.

Supplementary Material 1: Table S1. ***Cucurbita moschata*** accessions and stem color associated SNPs identified by GWAS and annotated genes. A threshold of -log10(p)=5 was used for the significant association detection of SNPs.

Supplementary Material 2: Table S2. qRT-PCR validated genes and primer sequences.

Supplementary Material 3: Table S3. Gene identifications from transcriptome analysis.

Supplementary Material 4: Table S4. Comparative transcriptome analysis of gene expression between mature yellow stems S2 and mature green stems S1.

Supplementary Material 5: Table S5. Comparative transcriptome analysis of gene expression between mature yellow stems S3 and mature green stems S1.

Supplementary Material 6: Table S6. Comparative transcriptome analysis of gene expression between young yellow stems YS2 and young green stems YS1.

Supplementary Material 7: Table S7. Comparative transcriptome analysis of gene expression between young yellow stems YS3 and young green stems YS1.

Supplementary Material 8: Table S8. DEGs regulated in different yellow stems (S2 vs S1, S3 vs S1, YS2 vs YS1 and YS3 vs YS1).

Supplementary Material 9: Table S9. Comparative transcriptome analysis of gene expression between mature green stems S1 and young green stems YS1.

Supplementary Material 10: Table S10. Comparative transcriptome analysis of gene expression between mature yellow stems S2 and young yellow stems YS2.

Supplementary Material 11: Table S11. Comparative transcriptome analysis of gene expression between mature yellow stems S3 and young yellow stems YS3.

Supplementary Material 12: Table S12. The highly correlated genes clustered in the blue module by WGCNA analysis using the expression values of the GWAS-identified candidates.

Supplementary Material 13: Table S13. The highly correlated genes clustered in the turquoise module by WGCNA analysis using the expression values of the GWAS-identified candidates.

Supplementary Material 14: Table S14. The highly correlated genes clustered in the yellow module by WGCNA analysis using the expression values of the GWAS-identified candidates.

Supplementary Material 15: Table S15. The highly correlated genes clustered in the brown module by WGCNA analysis using the expression values of the GWAS-identified candidates.

Supplementary Material 16

Author contributions
LTD: Conceptualization, Methodology, Investigation, Data curation, Visualization, Writing– original draft, Writing– review & editing. JNL: Methodology, Writing– review & editing. HBW: Software, Writing– review & editing. XXL: Software. GJZ: Methodology. HG: Writing– review & editing. XMZ: Writing– review & editing. CQN: Methodology, Data curation, Visualization. XTW: Methodology, Data curation. JXL: Conceptualization, Resources, Supervision, Methodology, Investigation, Writing– review & editing.

Funding
This work was supported by the Seed Industry Revitalization Project of Special Fund for Rural Revitalization Strategy of Gunagdong Province (grant number 2024-440400-103010206-0002); the Special Fund for Scientific Innovation Strategy-Construction of High Level Academy of Agriculture Science [grant number R2022YJ-YB1001]; the Science and Technology Innovation Strategy (Agricultural Research Main Force Construction) Project [grant number R2023PY-JX006]; the Guangzhou Science and Technology Planning Project [grant number 2023A04J0821]; and the Open Research Fund of Guangdong Key Laboratory for New Technology Research on Vegetables [grant number 2021KF-01]; the Guangdong Province Modern Vegetable Industry Technology System Project [grant number 2024CXTD08]; the National Bulk Vegetable Industry Technology System Guangzhou Comprehensive Experimental Station [grant number CARS-23-G50].

Data availability
Sequencing data is available on CNGB Sequence Archive (CNSA) of China National Genebank DataBase (CNGBdb) with accession number CNP0006173.

Declarations

Ethics approval and consent to participate
Not applicable.

Consent for publication
Not applicable.

Competing interests
The authors declare no competing interests.

Received: 17 January 2025 / Accepted: 5 May 2025
Published online: 23 May 2025

References

1. Pogson BJ, Albrecht V. Genetic dissection of chloroplast biogenesis and development: an overview. Plant Physiol. 2011;155(4):1545–51.
2. Wang P, Grimm B. Connecting chlorophyll metabolism with accumulation of the photosynthetic apparatus. Trends Plant Sci. 2021;26(5):484–95.
3. Munoz P, Munne-Bosch S. Photo-oxidative stress during leaf, flower and fruit development. Plant Physiol. 2018;176(2):1004–14.
4. Sathasivam R, Radhakrishnan R, Kim JK, Park SU. An update on biosynthesis and regulation of carotenoids in plants. South Afr J Bot. 2021;140:290–302.
5. Wang Y, Ma Q, Lin L, Zhang H, Luo X, Wang J, Lv X, Deng Q. Integrated cytological, physiological, and transcriptome analysis of the bud mutant of jujube (ziziphus jujuba mill.) with non-lethal albino phenotype. Ind Crops Prod. 2023;201:116964.
6. Peng H, Gao J, song X. Transcriptome analyses reveal photosynthesis-related genes involved in chloroplast development of the EMS-induced maize mutant. Plant Biotechnol Rep. 2022;16(5):565–78.
7. Li J, Jia X, Liu L, Cao X, Xiong Y, Yang Y, Zhou H, Yi M, Li M. Comparative biochemical and transcriptome analysis provides insights into the regulatory mechanism of striped leaf albinism in arecanut (areca catechu L). Ind Crops Prod. 2020;154:112734.
8. Lichtenthaler HK. Plastoglobuli, thylakoids, chloroplast structure and development of plastids. In: Plastid Development in Leaves during Growth and Senescence. Edited by Biswal B, Krupinska K, Biswal UC. Dordrecht: Springer Netherlands; 2013;36:337–61.
9. Dubreuil C, Jin X, Barajas-López JD, Hewitt TC, Tanz SK, Dobrenel T, Schröder WP, Hanson J, Pesquet E, Grönlund A, et al. Establishment of photosynthesis through chloroplast development is controlled by two distinct regulatory phases. Plant Physiol. 2018;176(2):1199–214.
10. Wang X, An Y, Xu P, Xiao J. Functioning of PPR proteins in organelle RNA metabolism and chloroplast biogenesis. Front Plant Sci. 2021;12:627501.
11. Hristou A, Gerlach I, Stolle DS, Neumann J, Bischoff A, Dunschede B, Nowaczyk MM, Zoschke R, Schunemann D. Ribosome-associated chloroplast SRP54 enables efficient cotranslational membrane insertion of key photosynthetic proteins. Plant Cell. 2019;31(11):2734–50.
12. Manuell AL, Quispe J, Mayfield SP. Structure of the chloroplast ribosome: novel domains for translation regulation. PLoS Biol. 2007;5(8):e209.
13. Bieri P, Leibundgut M, Saurer M, Boehringer D, Ban N. The complete structure of the chloroplast 70S ribosome in complex with translation factor pY. EMBO J. 2017;36(4):475–86.
14. Mahapatra K, Mukherjee A, Suyal S, Dar MA, Bhagavatula L, Datta S. Regulation of chloroplast biogenesis, development, and signaling by endogenous and exogenous cues. Physiol Mol Biology Plants. 2024;30(2):167–83.
15. Zhu X, Chen J, Qiu K, Kuai B. Phytohormone and light regulation of chlorophyll degradation. Front Plant Sci. 2017;8:1911.
16. Batool M, Ranjha M, Roobab U, Manzoor MF, Farooq U, Nadeem HR, Nadeem M, Kanwal R, AbdElgawad H, Al Jaouni SK et al. Nutritional value, phytochemical potential, and therapeutic benefits of pumpkin (Cucurbita sp). Plants (Basel). 2022;11(11).
17. Deng L, Yang X, Qiu Y, Luo J, Wu H, Liu X, Zhao G, Gong H, Zheng X, Li J. Metabolic and molecular mechanisms underlying the foliar Zn application induced increase of 2-acetyl-1-pyrroline conferring the 'taro-like' aroma in pumpkin leaves. Front Plant Sci. 2023;14:1127032.
18. Lippert C, Listgarten J, Liu Y, Kadie CM, Davidson RI, Heckerman D. FaST linear mixed models for genome-wide association studies. Nat Methods. 2011;8(10):833–5.
19. Langfelder P, Horvath S. WGCNA: an R package for weighted correlation network analysis. BMC Bioinformatics. 2008;9:559.
20. Shi C, Shen X, Zhang Z, Zhou Y, Chen R, Luo J, Tang Y, Lu Y, Li F, Ouyang B. Conserved role of fructokinase-like protein 1 in chloroplast development revealed by a seedling-lethal albino mutant of pepper. Hortic Res. 2022;9.
21. Kusaba M, Ito H, Morita R, Iida S, Sato Y, Fujimoto M, Kawasaki S, Tanaka R, Hirochika H, Nishimura M, et al. Rice NON-YELLOW COLORING1 is involved in light-harvesting complex II and grana degradation during leaf senescence. Plant Cell. 2007;19(4):1362–75.
22. Sakuraba Y, Jeong J, Kang MY, Kim J, Paek NC, Choi G. Phytochrome-interacting transcription factors PIF4 and PIF5 induce leaf senescence in Arabidopsis. Nat Commun. 2014;5:4636.
23. Wang Y, Ren Y, Zhou K, Liu L, Wang J, Xu Y, Zhang H, Zhang L, Feng Z, Wang L, et al. WHITE STRIPE LEAF4 encodes a novel P-Type PPR protein required for chloroplast biogenesis during early leaf development. Front Plant Sci. 2017;8:1116.
24. Li WX, Yang SB, Lu Z, He ZC, Ye YL, Zhao BB, Wang L, Jin B. Cytological, physiological, and transcriptomic analyses of golden leaf coloration in Ginkgo biloba L. Hortic Res. 2018;5:32.
25. Austin JR, Frost E, Vidi P-A, Kessler F, Staehelin LA. Plastoglobules are lipoprotein subcompartments of the chloroplast that are permanently coupled to thylakoid membranes and contain biosynthetic enzymes. Plant Cell. 2006;18(7):1693–703.
26. Michel EJS, Ponnala L, van Wijk KJ. Tissue-type specific accumulation of the plastoglobular proteome, transcriptional networks, and plastoglobular functions. J Exp Bot. 2021;72(13):4663–79.
27. Shanmugabalaji V, Zita W, Collombat J, Kessler F. Chapter three - plastoglobules: a hub of lipid metabolism in the chloroplast. In: Advances in Botanical Research. Edited by Rébeillé F, Maréchal E, vol. 101: Academic Press; 2022:91–119.
28. Harpaz-Saad S, Azoulay T, Arazi T, Ben-Yaakov E, Mett A, Shiboleth YM, Hörtensteiner S, Gidoni D, Gal-On A, Goldschmidt EE, et al. Chlorophyllase is a rate-limiting enzyme in chlorophyll catabolism and is posttranslationally regulated. Plant Cell. 2007;19(3):1007–22.
29. Ren G, An K, Liao Y, Zhou X, Cao Y, Zhao H, Ge X, Kuai B. Identification of a novel chloroplast protein AtNYE1 regulating chlorophyll degradation during leaf senescence in Arabidopsis. Plant Physiol. 2007;144(3):1429–41.
30. Zhou F, Wang CY, Gutensohn M, Jiang L, Zhang P, Zhang D, Dudareva N, Lu S. A recruiting protein of geranylgeranyl diphosphate synthase controls metabolic flux toward chlorophyll biosynthesis in rice. Proceedings of the National Academy of Sciences. 2017;114(26):6866–6871.
31. Zhang X, Wen B, Zhang Y, Li Y, Yu C, Peng Z, Wang K, Liu Z, Huang J-a, Xiong L, et al. Transcriptomic and biochemical analysis reveal differential regulatory

mechanisms of photosynthetic pigment and characteristic secondary metabolites between high amino acids green-leaf and albino tea cultivars. Sci Hort. 2022;295:110823.
32. Ohmiya A, Kishimoto S, Aida R, Yoshioka S, Sumitomo K. Carotenoid cleavage dioxygenase (CmCCD4a) contributes to white color formation in chrysanthemum petals. Plant Physiol. 2006;142(3):1193–201.
33. Zaidi S, Arif Y, Imtiaz H, Shiraz M, Hayat S. Structural chemistry, biosynthesis, and signaling of multifaceted plant growth regulator: strigolactone. J Plant Growth Regul. 2024;43(8):2489–502.
34. Walter MH, Strack D. Carotenoids and their cleavage products: biosynthesis and functions. Nat Prod Rep. 2011;28(4):663–92.
35. Manara A, DalCorso G, Leister D, Jahns P, Baldan B, Furini A. AtSIA1 and AtOSA1: two Abc1 proteins involved in oxidative stress responses and iron distribution within chloroplasts. New Phytol. 2014;201(2):452–65.
36. Lundquist PK, Poliakov A, Giacomelli L, Friso G, Appel M, McQuinn RP, Krasnoff SB, Rowland E, Ponnala L, Sun Q, et al. Loss of plastoglobule kinases ABC1K1 and ABC1K3 causes conditional degreening, modified prenyl-lipids, and recruitment of the jasmonic acid pathway. Plant Cell. 2013;25(5):1818–39.
37. Wang G, Zeng F, Song P, Sun B, Wang Q, Wang J. Effects of reduced chlorophyll content on photosystem functions and photosynthetic electron transport rate in rice leaves. J Plant Physiol. 2022;272:153669.
38. Yamauchi N, Funamoto Y, Shigyo M. Peroxidase-mediated chlorophyll degradation in horticultural crops. Phytochem Rev. 2004;3(1):221–8.
39. Sun Y, Li J, Zhang L, Lin R. Regulation of chloroplast protein degradation. J Genet Genomics. 2023;50(6):375–84.
40. Paraskevopoulos K, Kriegenburg F, Tatham MH, Roesner HI, Medina B, Larsen IB, Brandstrup R, Hardwick KG, Hay RT, Kragelund BB, et al. Dss1 is a 26S proteasome ubiquitin receptor. Mol Cell. 2014;56(3):453–61.
41. Sun Y, Yao Z, Ye Y, Fang J, Chen H, Lyu Y, Broad W, Fournier M, Chen G, Hu Y, et al. Ubiquitin-based pathway acts inside chloroplasts to regulate photosynthesis. Sci Adv. 2022;8(46):eabq7352.
42. Tanaka K. The proteasome: overview of structure and functions. Proc Japan Acad Ser B Phys Biol Sci. 2009;85(1):12–36.
43. Richau KH, Kaschani F, Verdoes M, Pansuriya TC, Niessen S, Stüber K, Colby T, Overkleeft HS, Bogyo M, Van der Hoorn RAL. Subclassification and biochemical analysis of plant papain-like cysteine proteases displays subfamily-specific characteristics. Plant Physiol. 2012;158(4):1583–99.
44. Turk V, Stoka V, Vasiljeva O, Renko M, Sun T, Turk B, Turk D. Cysteine cathepsins: from structure, function and regulation to new frontiers. Biochim Biophys Acta. 2012;1824(1):68–88.
45. Frank S, Hollmann J, Mulisch M, Matros A, Carrion CC, Mock HP, Hensel G, Krupinska K. Barley cysteine protease PAP14 plays a role in degradation of chloroplast proteins. J Exp Bot. 2019;70(21):6057–69.
46. Eason JR, West PJ, Brummell DA, Watson LM, Somerfield SD, McLachlan ARG. Overexpression of the protease inhibitor BoCPI-1 in broccoli delays chlorophyll loss after harvest and causes down-regulation of cysteine protease gene expression. Postharvest Biol Technol. 2014;97:23–31.
47. Yildiz A. Mechanism and regulation of kinesin motors. Nat Rev Mol Cell Biol. 2024;26:86–103.
48. Ali I, Yang WC. The functions of kinesin and kinesin-related proteins in eukaryotes. Cell Adhes Migr. 2020;14(1):139–52.
49. Suetsugu N, Yamada N, Kagawa T, Yonekura H, Uyeda TQ, Kadota A, Wada M. Two kinesin-like proteins mediate actin-based chloroplast movement in Arabidopsis thaliana. Proc Natl Acad Sci U S A. 2010;107(19):8860–5.
50. Hu B, Chen W, Guo L, Liu Y, Pu Z, Zhang G, Tu B, Yuan H, Wang Y, Ma B, et al. Characterization of a novel allele of bc12/gdd1 indicates a differential leaf color function for BC12/GDD1 in indica and japonica backgrounds. Plant Sci. 2020;298:110585.
51. Boex-Fontvieille E, Jossier M, Davanture M, Zivy M, Hodges M, Tcherkez G. Differential protein phosphorylation regulates chloroplast movement in response to strong light and darkness in Arabidopsis thaliana. Plant Mol Biology Report. 2014;32(5):987–1001.
52. Kumari D, Ray K. Phosphoregulation of kinesins involved in long-range intracellular transport. Front Cell Dev Biology. 2022;10:873164.
53. Szewinska J, Siminska J, Bielawski W. The roles of cysteine proteases and phytocystatins in development and germination of cereal seeds. J Plant Physiol. 2016;207:10–21.
54. Gonzalez-Calle V, Iglesias-Fernandez R, Carbonero P, Barrero-Sicilia C. The BdGAMYB protein from Brachypodium distachyon interacts with BdDOF24 and regulates transcription of the BdCathB gene upon seed germination. Planta. 2014;240(3):539–52.
55. Chen N, Pan L, Yang Z, Su M, Xu J, Jiang X, Yin X, Wang T, Wan F, Chi X. A MYB-related transcription factor from peanut, AhMYB30, improves freezing and salt stress tolerance in transgenic Arabidopsis through both DREB/CBF and ABA-signaling pathways. Front Plant Sci. 2023;14.
56. Lian WH, Sun TX, Meng XY, Sun R, Hui F, Jiang YN, Zhao Y. Overexpression of the Panax ginseng MYB4 gene enhances stress tolerance in transgenic Arabidopsis thaliana. Biol Plant. 2021;65:27–38.
57. Lu X, Yang L, Yu M, Lai J, Wang C, McNeil D, Zhou M, Yang C. A novel Zea mays Ssp. mexicana L. MYC-type ICE-like transcription factor gene ZmmICE1, enhances freezing tolerance in transgenic Arabidopsis thaliana. Plant Physiol Biochem. 2017;113:78–88.

Publisher's note